

Structural, Magnetic and Catalytic Properties of a New Vacancy Ordered Perovskite Type Barium Cobaltate $\text{BaCoO}_{2.67}$

Aamir Iqbal Waidha,^[a] Humera Khatoon Siddiqui,^[b] Yuji Ikeda,^[c] Maren Lepple,^[d] Sami Vasala,^[a] Manuel Donzelli,^[a] A. D. Fortes,^[e] Peter Slater,^[f] Blazej Grabowski,^[c] Ulrike I. Kramm,^[b] and Oliver Clemens*^[a]

Abstract: A new vacancy ordered, anion deficient perovskite modification with composition of $\text{BaCoO}_{2.67}$ ($\text{Ba}_3\text{Co}_3\text{O}_8\Box_1$) has been prepared via a two-step heating process. Combined Rietveld analysis of neutron and X-ray powder diffraction data shows a novel ordering of oxygen vacancies not known before for barium cobaltates. A combination of neutron powder diffraction, magnetic measurements, and density functional theory (DFT) studies confirms G-type antiferromagnetic ordering. From impedance measurements, the electronic conductivity of the order of 10^{-4} Scm^{-1} is determined. Remarkably, the bifunctional catalytic activity for oxygen evolution reaction (OER) and oxygen reduction reaction (ORR) is found to be comparable to that of $\text{Ba}_{0.5}\text{Sr}_{0.5}\text{Co}_{0.8}\text{Fe}_{0.2}\text{O}_{3-y}$, confirming that charge-ordered anion deficient non-cubic perovskites can be highly efficient catalysts.

Perovskite-type ABX_{3-y} compounds have received a lot of attention due to their application in the fields of magnetism, fuel cells, solar cells and batteries.^[1] The ideal perovskite structure (ABX_3) can be described as a cubic close packed (*ccp*) arrangement of AX_3 layers with *B* sites occupying $1/4$ of octahedral voids resulting in a corner sharing octahedral network. The anion sublattice in such a structure is highly

flexible and can accommodate a large amount of vacancies (ABX_{3-y} , $y=1$ being reported^[2]), which can result in enhanced electronic conductivity due to mixed valency of the *B* site cation, which forms an important prerequisite towards developing perovskite catalysts for OER/ORR for fuel cell applications.^[3] In this respect, cobalt-containing perovskites have been of particular interest due to their catalytic, magnetic and electronic properties.^[3–4]

For BaCoO_{3-y} systems, a variety of compounds have been reported and summarized depending on the value of *y* by Raveau et al.^[1] and Mentré et al.^[5] For oxygen rich systems, i.e. for low values of *y*, hexagonal modifications (2H, 5H, 12H) are known and for higher values of *y*, the cubic modification or *ccp*-related vacancy-ordered variants are known ($\text{BaCoO}_{2.22}$ and BaCoO_2),^[2,5–6] and *ccp*-related arrangements can also be stabilized by the uptake of water ($\text{BaCoO}_{1.80}(\text{OH})_{0.86}$).^[7] Such or similar barium cobaltates have attracted a lot of attention for their activity for the oxygen evolution reaction (OER).^[8]

Herein, we report a new vacancy ordered *ccp*-related modification of barium cobaltate with a composition of $\text{BaCoO}_{2.67}$ ($\text{Ba}_3\text{Co}_3\text{O}_8\Box_1$, \Box = anion vacancy) prepared by a two-step heating process together with its electrocatalytic and magnetic properties. The heating steps, times and temperatures were found to be of significant importance for the successful synthesis of the title compound. After the first heating step at 1273 K for 60 h under a flow of argon gas, X-ray powder diffraction data indicate the formation of a barium cobaltate

[a] A. Iqbal Waidha, Dr. S. Vasala, M. Donzelli, Dr. O. Clemens
Materials Synthesis Group
Institute of Material Science
University of Stuttgart
Hesisenbergstraße 3, 70569 Stuttgart (Germany)
E-mail: oliver.clemens@imw.uni-stuttgart.de

[b] H. Khatoon Siddiqui, Dr. U. I. Kramm
Catalysts and Electrocatalyst
Department of Chemistry
Eduard-Zintl Institute for Inorganic and Physical Chemistry
Technische Universität Darmstadt
64287 Darmstadt (Germany)

[c] Dr. Y. Ikeda, Dr. B. Grabowski
Department of Materials Design
Institute for Materials Science
University of Stuttgart
Pfaffenwaldring 55, 70569, Stuttgart (Germany)

[d] Dr. M. Lepple
DECHEMA-Forschungsinstitut
Theodor-Heuss-Allee 25, 60486 Frankfurt am Main (Germany)

[e] Dr. A. D. Fortes
Rutherford Appleton Laboratory
Harwell Science and Innovation Campus
ISIS Facility
Didcot, Oxfordshire OX11 0QX (UK)

[f] Dr. P. Slater
School of Chemistry
University of Birmingham
Edgbaston, Birmingham B15 2TT (UK)

Supporting information for this article is available on the WWW under <https://doi.org/10.1002/chem.202101167>

© 2021 The Authors. Published by Wiley-VCH GmbH. This is an open access article under the terms of the Creative Commons Attribution License, which permits use, distribution and reproduction in any medium, provided the original work is properly cited.

phase with a diffraction pattern similar to the vacancy-ordered monoclinic modification of $\text{BaFeO}_{2.5}$ ^[9] together with an additional tetragonal perovskite type phase (see Figure S1 in Supporting Information). Unfortunately, this phase could not be obtained in a pure form. From the energy dispersive X-ray spectroscopic analysis (EDX), a 1:1 ratio of Ba:Co was confirmed (Figure S2 in Supporting Information), and iodometric titrations on this phase mixture indicated an average oxidation state of +2.93(1) for cobalt, implying an overall average composition of $\text{BaCoO}_{2.46}$. In order to determine the topochemical oxidation behavior of this compound and suitable reaction conditions for oxygen uptake, simultaneous thermal analysis (STA, see Figure S3 in Supporting Information) was carried out in oxygen atmosphere, which showed an onset of oxygen uptake at 455 K. This mass increase corresponds to an uptake of ~ 0.21 moles of oxygen, which means an average oxidation state of 3.34 for cobalt and a composition corresponding to $\sim \text{BaCoO}_{2.67}$. Iodometric titrations confirmed this composition. At 535 K a second mass increase and oxygen uptake is observed, which would lead to a final composition of $\text{BaCoO}_{2.80}$. The underlying phase changes were investigated by temperature dependent XRD measurements starting from the phase mixture with composition of $\text{BaCoO}_{2.46}$ obtained after the first heating step in oxygen atmosphere. Changes in diffraction pattern are observed starting at 448 K (Figure S4a in Supporting Information). At 473 K, the X-ray diffractogram shows the appearance of a single phase of the title compound (Figure S4b

in Supporting Information), whereas the patterns recorded at 573 K and above show the presence of a hexagonal-type modification (Figure S4c in Supporting Information), which agrees well with the further oxygen uptake observed in STA. The appearance of this hexagonal phase is in close agreement to what was reported previously by Raveau et al.^[1]

To determine the structure and phase composition of the new modification with composition $\text{BaCoO}_{2.67}$, a larger batch of this material was prepared from the as-determined optimized reaction conditions of the second heating step and X-ray diffraction as well as neutron diffraction data were recorded and analyzed, see Figure 1. The diffraction pattern showed principle similarity to the cubic perovskite modification with apparent splitting of the main reflections and appearance of superstructure reflections. All the reflections could be indexed with a monoclinic unit cell with $a = 10.1718(3)$ Å, $b = 5.6035(2)$ Å, $c = 6.9248(2)$ Å and $\beta = 91.465(4)^\circ$, where the lengths of the axes indicate a $\sqrt{6} \times \sqrt{2} \times \sqrt{3}$ supercell of the cubic aristotype structure (we note that $\sim 3.23(1)$ wt% of CoO were found as impurity for the larger batch, which indicates close to full homogeneity of the powder). Pawley fits indicated the centrosymmetric monoclinic space group $P2_1/m$ as the most likely symmetry in agreement with the missing (0 1 0) reflection, which is forbidden and could be observed neither in the X-ray nor the neutron diffraction data, further indicating the presence of the 2_1 screw axis (see Figure S5 in Supporting Information for the structural relationship). This symmetry had been previously

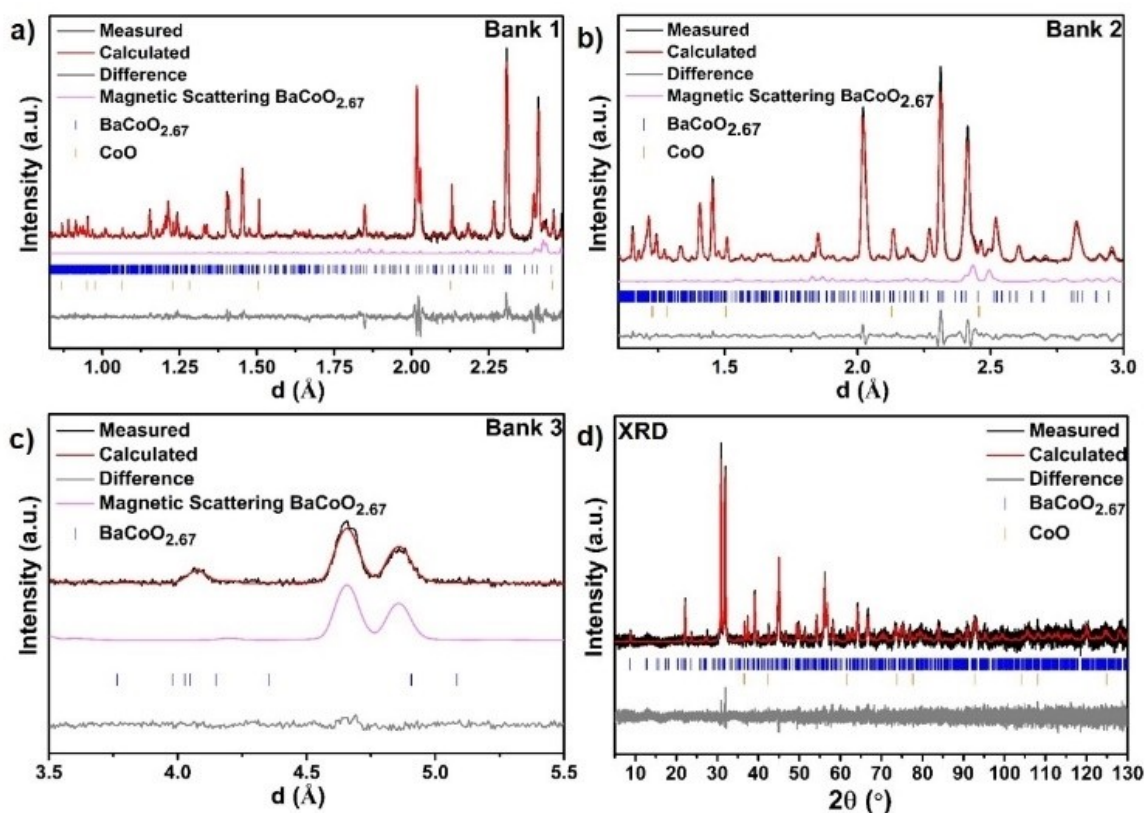


Figure 1. Coupled Rietveld analysis of the room temperature neutron (HRPD, bank 1–3, a–c) and X-ray diffraction (d) patterns recorded for $\text{BaCoO}_{2.67}$.

found for the compound $\text{BaFeO}_{2.33}\text{F}_{0.33}$ ^[10,11] with similar overall anion composition by our group for which the symmetry lowering was found to originate from ordering of the anion vacancies. Another member, $\text{BaFeO}_{2.67}$, of the $\text{Ba}(\text{Fe},\text{Co})(\text{O},\text{F})_{2.67}$ family was recently prepared, and it appears to be isotypic to both $\text{BaFeO}_{2.33}\text{F}_{0.33}$ and $\text{BaCoO}_{2.67}$, which we will report in a separate article. The structural similarity between these compounds is plausible since they contain similar overall anion contents showing that in the setting of a barium-rich anion-deficient perovskite lattice, only certain anion compositions can give highly favorable structural stabilization and in agreement with our previous finding that hydrated barium ferrates and cobaltates possess close structural similarity.^[2–3,7,12] Therefore, the structural model of $\text{BaFeO}_{2.33}\text{F}_{0.33}$ suggested by Clemens et al.^[11] was used as the starting model (see Table S1 in Supporting Information for the starting model) for the structural analysis of the X-ray and neutron diffraction data. Relaxation of the model resulted in an excellent fitting of the diffraction data with chemically plausible structural model (see bond distances in Table S5 provided in Supporting Information). Similar to $\text{BaFeO}_{2.33}\text{F}_{0.33}$, the $2a$ anion site was found to be vacant which, in combination with smaller structural relaxations, gives rise to cobalt being present in three different coordination environments, i.e., tetrahedral, square pyramidal and octahedral (see Table S2 in Supporting Information for the refined structural model and Figure 2 structural schematics). Compared to $\text{BaFeO}_{2.33}\text{F}_{0.33}$, wherein the Fe cations are only present in the

trivalent oxidation state, $\text{BaCoO}_{2.67}$ contains mixed valent B site as determined from iodometric titrations corresponding to +3 and +4 oxidation states. From the structural refinements, the average Co–O distances of 2.02 Å, 1.79 Å and 2.01 Å for 6-, 5- and 4-fold coordination were determined for Co1, Co2 and Co3 respectively, which indicates an oxidation state of +3 for Co1 and Co3, as well as +4 for the Co2 site from a consideration of average bond distance,^[13] and a calculation of bond valence sums (see Table S6 in Supporting Information). We also would like to acknowledge that we attempted to refine the structure in non-centrosymmetric monoclinic subgroups or within the triclinic subgroup $P-1$. Since these models did not result in any significant improvement of the fit, they were discarded.

Field dependent measurements of magnetization ($M-H$) were recorded at 10, 80, 250 and 320 K (Figure 3a), which mainly indicated an antiferromagnetic behavior with only a small residual ferromagnetic moment at 10 K ($\sim 0.00003 \mu_B$). This is in agreement with field and zero field cooled measurements (Figure 3b) which showed a small but significant difference. This ferromagnetic contribution could be due to the presence of impurity or magnetic canting, which would be undeterminable via powder diffraction techniques. The anti-

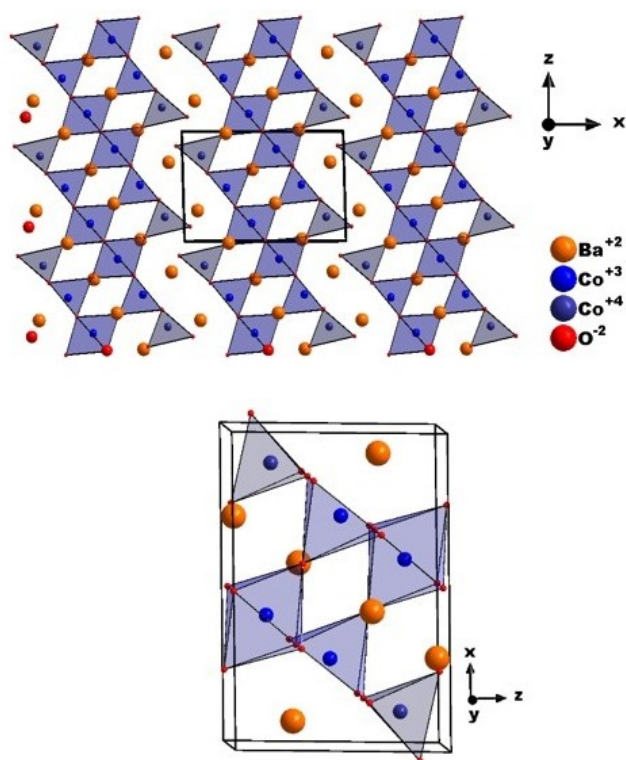


Figure 2. Refined crystal structure of $\text{BaCoO}_{2.67}$ obtained from the coupled Rietveld fit of neutron and X-ray diffraction data showing the vacancy ordering and three different Co coordination environments.

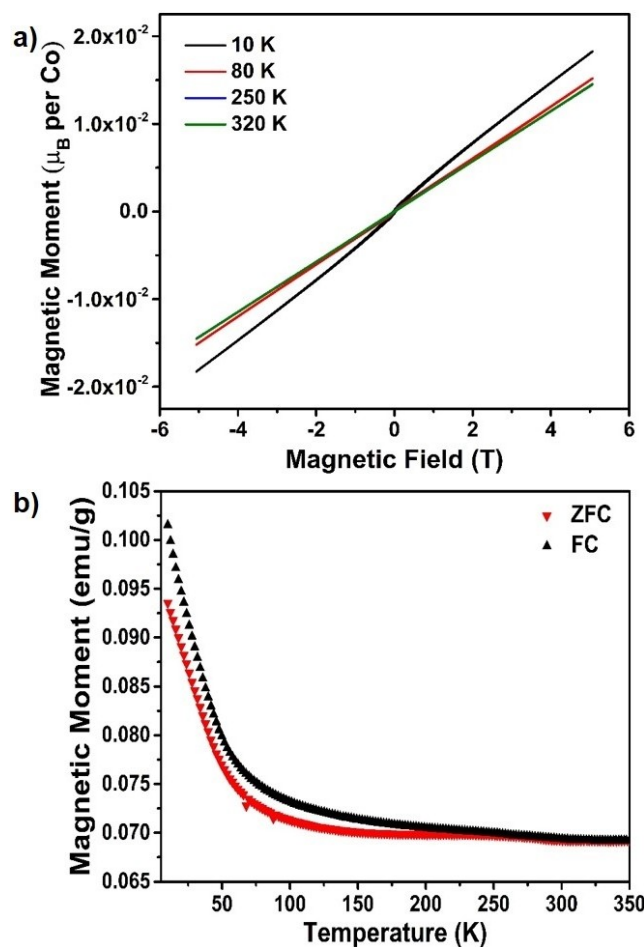


Figure 3. a) Field dependent measurements of magnetization of $\text{BaCoO}_{2.67}$. b) Temperature dependent measurements of magnetization for zero-field cooled and field-cooled sample of $\text{BaCoO}_{2.67}$.

ferromagnetic ordering below 350 K is further indicated by the presence of magnetic reflections in the neutron powder diffraction patterns measured at ambient temperatures. These magnetic reflections indicate a magnetic k -vector of $[0\ 0\ \frac{1}{2}]$. Thus we attempted to refine the magnetic intensity with different structural models, and found that it can be best described with a G-type antiferromagnetic structure with an average magnetic moment of $2.36(1)\ \mu_B$ aligned along the c -axis. The magnetic moment obtained from the refinements suggests an intermediate spin state for Co with ~ 1 – 2 unpaired electrons on average. Density functional theory (DFT) based calculations also found consistently that the G-type antiferromagnetically ordered state (G-AFM) is energetically more favorable than the ferromagnetic (FM) state, which nicely supports the experiments above (Figure S6 in Supporting Information).

Electrochemical impedance spectroscopy measurements (Figure S7 in Supporting Information) were carried out to determine the conductivity of the sample. From the NYQUIST plot a single depressed semicircle was observed which was fitted using a single R-CPE (constant phase element). The room temperature conductivity of the sample was determined from the intercept on the X-axis and calculated to be $2.89 \times 10^{-4}\ \text{S cm}^{-1}$ which is of the same order of magnitude as that of $\text{BaCoO}_{1.80}(\text{OH})_{0.86}$ ^[7] and three orders of magnitude higher than that of $\text{BaCoO}_{2+\delta}$.^[2] This is in agreement with what is expected from the presence of Co in a mixed oxidation state ($+3/+4$). An activation energy of $0.21(1)\ \text{eV}$ was calculated from the slope of the Arrhenius plot (Figure 4a) indicating the dominance of electronic contribution to overall conductivity.^[2]

The catalytic activity for OER and ORR was measured for the title compound $\text{BaCoO}_{2.67}$ and compared to that of $\text{Ba}_{0.5}\text{Sr}_{0.5}\text{Co}_{0.8}\text{Fe}_{0.2}\text{O}_{3-y}$ (BSCF) which is the benchmark perovskite catalyst^[4,14] (see section 4 and Figures S8–S11 in Supporting Information for more details on preparation of reference electrodes and comparative morphological as well as electrochemical characterization). The catalytic activity in the absence of carbon is low for both compounds (see Figures S10 and S11). Referencing the activity data to the surface area of the perovskites (Figure S10c and d) indicate similar onset of both materials for the ORR while the overall current density (per BET surface area) is larger for $\text{Ba}_{0.5}\text{Sr}_{0.5}\text{Co}_{0.8}\text{Fe}_{0.2}\text{O}_{3-y}$. The performance towards OER is much better for $\text{Ba}_{0.5}\text{Sr}_{0.5}\text{Co}_{0.8}\text{Fe}_{0.2}\text{O}_{3-y}$ which might be related to the integration of iron in the system, as it is known for several OER catalysts.^[15]

Once carbon is added, the catalytic activity of the title compound is very similar to that of the BSCF (for reasons of comparability, the OER and ORR data are plotted together and are shown in Figure 4b), though the $\text{BaCoO}_{2.67}$ particles showed a much coarser crystallinity (see Figure S9 in Supporting Information). From the ORR region, we see that the potential of $0.7\ \text{V}$ vs. RHE (reversible hydrogen electrode) a kinetic current density of $2.3\ \text{mA cm}^{-2}$ is achieved and an onset potential of $0.81\ \text{V}$ for $\text{BaCoO}_{2.67}$. On the other hand, BSCF shows a kinetic current density of $2.1\ \text{mA cm}^{-2}$ at $0.7\ \text{V}$ with the onset potential of $0.785\ \text{V}$. The positive shift of the onset potential and larger

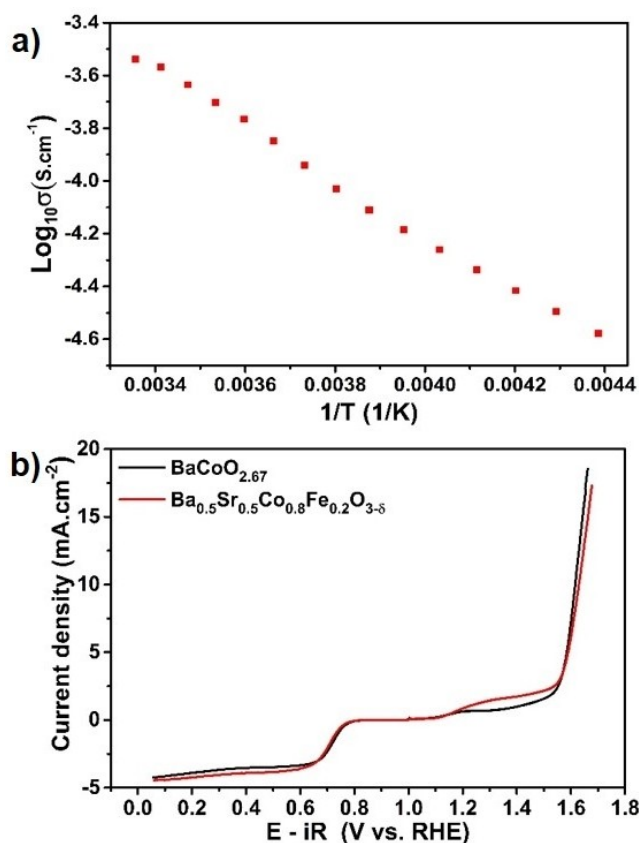


Figure 4. a) Arrhenius plot for $\text{BaCoO}_{2.67}$ measured in the temperature range of 228 to 298 K. b) Comparison of ORR/OER activity between $\text{BaCoO}_{2.67}$ and BSCF in 0.1 M KOH. For ORR and OER the cathodic and anodic sweep are displayed, respectively.

current density therefore indicate a slightly better ORR activity for $\text{BaCoO}_{2.67}$ as compared to BSCF.

In addition to ORR we also investigated the OER characteristics of both $\text{BaCoO}_{2.67}$ and BSCF. With the addition of carbon both compounds show almost similar onset potentials and achieve the benchmarking value of $10\ \text{mA cm}^{-2}$ at similar potential. The Tafel slopes of both samples are higher in comparison to literature values^[16] (see Figure S12 and Table S7 in Supporting Information). The origin of this, might be found in smaller conductivity or a larger grain size of our samples in comparison to those investigated in the literature. The bifunctional performance ($\Delta U = U_{\text{OER}} - U_{\text{ORR}}$) was calculated to be $0.95\ \text{V}$ for both $\text{BaCoO}_{2.67}$ and BSCF which is much lower compared to the $\text{BaFe}_{1-x}\text{Co}_x\text{O}_{3-y-\delta}(\text{OH})_y$ series^[3] and comparable to that of noble metal catalyst.^[17]

In relation to the suggested dependency of the catalytic activity on electron configuration as provided by Suntivich et al.,^[14,18] we aim to provide a qualitative reasoning why similarly high activity can be obtained for $\text{BaCoO}_{2.67}$ in comparison to BSCF, though no morphological optimization of the compound was performed. According to Suntivich et al.^[14,18] both ORR and OER activity are highly dependent on the e_g orbital filling of the transition metal ion with an average occupation of one electron being desirable. For mixed-valent

BaCoO_{2.67}, all Co ions are located in polyhedra with a local site symmetry of *m*. Such an average filling of e_g states is plausible if Co is present in the intermediate spin state. This would result in the electronic configuration of t_{2g}⁵e_g¹ for Co³⁺ (and high spin e_g³t_{2g}² for Co⁴⁺), which could be brought in principle agreement with the local symmetry and thus non-degeneracy within e_g/t_{2g} levels,^[1] and which might favor such similar catalytic activity. For BSCF, Co has been reported to be present in the intermediate state which would result in the likely electronic configuration of t_{2g}⁵e_g^{~1.25} (average Co oxidation state of +2.75 determined from iodometric titrations).^[14] In addition to the impact of the ordered coordination environments and their impact on the electronic configurations, this results in a high density of states (DOS) near the Fermi level for both BSCF and BaCoO_{2.67} (Figure S11). Although determining the exact spin state of Co in BaCoO_{2.67} on the different crystallographic sites with octahedral, square pyramidal, or tetragonal coordination is hindered experimentally, the catalytic activity observed here in combination with the magnetic moment observed at room temperature by neutron diffraction is plausible in relation to electron configurations found in similar compounds, with an overall occupation of the higher *d*-orbital energy levels by 1.33 electrons for BaCoO_{2.67}. Thus, ordering of vacancies can be considered to be the origin for the resulting ordering of charges and electron configurations, which in turn contribute to achieve a high catalytic activity in BaCoO_{2.67}.

Acknowledgements

We gratefully acknowledge awarding of beam time from the STFC (DOI: 10.5286/ISIS.E.87849379). O. Clemens acknowledges funding by DFG within CL551/2-1.H.K.S. and U.I.K. acknowledge financial support by the Hessian State Ministry for Higher Education, Research and Arts under the LOEWE collaborative project "FLAME". Open access funding enabled and organized by Projekt DEAL.

Conflict of Interest

The authors declare no conflict of interest.

Keywords: ab initio calculations · bifunctional catalyst · magnetism · neutron diffraction · perovskite

- [1] B. Raveau, M. Seikh, *Cobalt Oxides: From Crystal Chemistry to Physics*, Wiley VCH, Weinheim, 2012, p. 3–70.
- [2] A. I. Waidha, H. Zhang, M. Lepple, S. Dasgupta, L. Alff, P. Slater, A. D. Fortes, O. Clemens, *Chem. Commun.* 2019, 55, 2920–2923.
- [3] A. I. Waidha, L. Ni, J. Ali, M. Lepple, M. Donzelli, S. Dasgupta, S. Wollstadt, L. Alff, U. I. Kramm, O. Clemens, *J. Mater. Chem. A* 2020, 8, 616–625.
- [4] G. Chen, W. Zhou, D. Guan, J. Sunarso, Y. Zhu, X. Hu, W. Zhang, Z. Shao, *Sci. Adv.* 2017, 3, e1603206.
- [5] O. Mentre, M. Iorgulescu, M. Huve, H. Kabbour, N. Renaut, S. Daviero-Minaud, S. Colis, P. Roussel, *Dalton Trans.* 2015, 44, 10728–10737.
- [6] U. Spitsbergen, *Acta Crystallogr.* 1960, 13, 197–198.
- [7] A. I. Waidha, M. Lepple, K. Wissel, A. Benes, S. Wollstadt, P. R. Slater, A. D. Fortes, O. Clemens, *Dalton Trans.* 2018, 47, 11136–11145.
- [8] a) X. Xu, C. Su, W. Zhou, Y. Zhu, Y. Chen, Z. Shao, *Adv. Sci.* 2016, 3, 1500187; b) X. Xu, W. Wang, W. Zhou, Z. Shao, *Small Methods* 2018, 2, 1800071 –.
- [9] O. Clemens, M. Groting, R. Witte, J. M. Perez-Mato, C. Loho, F. J. Berry, R. Kruk, K. S. Knight, A. J. Wright, H. Hahn, P. R. Slater, *Inorg. Chem.* 2014, 53, 5911–5921.
- [10] O. Clemens, *J. Solid State Chem.* 2015, 225, 261–270.
- [11] O. Clemens, C. Reitz, R. Witte, R. Kruk, R. I. Smith, *J. Solid State Chem.* 2016, 243, 31–37.
- [12] T. Yamamoto, Y. Kobayashi, N. Hayashi, C. Tassel, T. Saito, S. Yamanaka, M. Takano, K. Ohoyama, Y. Shimakawa, K. Yoshimura, H. Kageyama, *J. Am. Chem. Soc.* 2012, 134, 11444–11454.
- [13] R. D. Shannon, *Acta Crystallogr. Sect. A* 1976, A32, 751–767.
- [14] J. Suntivich, K. J. May, H. A. Gasteiger, J. B. Goodenough, Y. Shao-Horn, *Science* 2011, 334, 1383–1385.
- [15] a) N. Weidler, S. Paulus, J. Schuch, J. Klett, S. Hoch, P. Stenner, A. Maljus, J. Brotz, C. Wittich, B. Kaiser, W. Jaegermann, *Phys. Chem. Chem. Phys.* 2016, 18, 10708–10718; b) D. Friebe, M. W. Louie, M. Bajdich, K. E. Sanwald, Y. Cai, A. M. Wise, M. J. Cheng, D. Sokaras, T. C. Weng, R. Alonso-Mori, R. C. Davis, J. R. Bargar, J. K. Norskov, A. Nilsson, A. T. Bell, *J. Am. Chem. Soc.* 2015, 137, 1305–1313; c) J. Schuch, S. Klemenz, P. Schuldt, A. M. Zieschang, S. Dolique, P. Connor, B. Kaiser, U. I. Kramm, B. Albert, W. Jaegermann, *ChemCatChem* 2021, 13, 1772–1780.
- [16] a) R. Mohamed, X. Cheng, E. Fabbri, P. Levecque, R. Kötz, O. Conrad, T. J. Schmidt, *J. Electrochem. Soc.* 2015, 162, F579–F586; b) Y. Zhu, W. Zhou, J. Yu, Y. Chen, M. Liu, Z. Shao, *Chem. Mater.* 2016, 28, 1691–1697.
- [17] Y. Gorlin, T. F. Jaramillo, *J. Am. Chem. Soc.* 2010, 132, 13612–13614.
- [18] J. Suntivich, H. A. Gasteiger, N. Yabuuchi, H. Nakanishi, J. B. Goodenough, Y. Shao-Horn, *Nat. Chem.* 2011, 3, 546–550.

Manuscript received: March 31, 2021

Accepted manuscript online: April 28, 2021

Version of record online: June 1, 2021